Available online at www.sciencedirect.com
SCIENCE DIRECT
Journal of Volcanology and Geothermal Research 143 (2005) 205–217
Journal of volcanology and geothermal research
www.elsevier.com/locate/jvolgeores

Bubble suspension rheology and implications for conduit flow

E.W. Llewellin[a,*], M. Manga[b]

[a]Department of Earth Sciences, University of Bristol, Wills Memorial Building, Queen's Road, Bristol, BS8 1RJ, UK
[b]University of California, Berkeley Seismological Laboratory, 215 McCone Hall #4760, Berkeley CA 94720-4760, USA

Received 5 February 2004; accepted 1 September 2004

Abstract

Bubbles are ubiquitous in magma during eruption and influence the rheology of the suspension. Despite this, bubble-suspension rheology is routinely ignored in conduit-flow and eruption models, potentially impairing accuracy and resulting in the loss of important phenomenological richness. The omission is due, in part, to a historical confusion in the literature concerning the effect of bubbles on the rheology of a liquid. This confusion has now been largely resolved and recently published studies have identified two viscous regimes: in regime 1, the viscosity of the two-phase (magma–gas) suspension increases as gas volume fraction ϕ increases; in regime 2, the viscosity of the suspension decreases as ϕ increases. The viscous regime for a deforming bubble suspension can be determined by calculating two dimensionless numbers, the capillary number Ca and the dynamic capillary number Cd.

We provide a didactic explanation of how to include the effect of bubble-suspension rheology in continuum, conduit-flow models. Bubble-suspension rheology is reviewed and a practical rheological model is presented, followed by an algorithmic, step-by-step guide to including the rheological model in conduit-flow models. Preliminary results from conduit-flow models which have implemented the model presented are discussed and it is concluded that the effect of bubbles on magma rheology may be important in nature and results in a decrease of at least 800 m in calculated fragmentation-depth and an increase of between 40% and 250% in calculated eruption-rate compared with the assumption of Newtonian rheology.

Keywords: magma rheology; bubble suspension; conduit-flow model; eruption model; capillary number

1. Introduction

The region between bubble nucleation and magma fragmentation in the volcanic conduit is characterized by the flow of a two-phase suspension of bubbles in magma (suspended crystals may also be present but are not considered in this paper). It is known from theory (e.g., Taylor, 1932; Mackenzie, 1950; Frankel and Acrivos, 1970), laboratory experiments (Bagdassarov and Dingwell, 1992, 1993; Stein and Spera, 1992, 2002; Lejeune et al., 1999; Rust and Manga, 2002a; Llewellin et al., 2002a), and numerical

* Corresponding author.
E-mail addresses: ed.llewellin@bris.ac.uk (E.W. Llewellin), manga@seismo.berkeley.edu (M. Manga).

0377-0273/$ - see front matter © 2005 Elsevier B.V. All rights reserved.
doi:10.1016/j.jvolgeores.2004.09.018

simulations (e.g., Manga et al., 1998; Manga and Loewenberg, 2001) that bubbles influence the rheology of the suspension. In particular, it is likely that the influence of bubbles on the shear viscosity of the magma ($\eta_s(\phi)$ where η_s is the viscosity of the bubble suspension and ϕ is the gas volume fraction) is an important control on conduit-flow and eruption dynamics. Despite this there has, until recently, been very little effort to include bubble suspension rheology in numerical conduit-flow models (but see Mastin, 2002, for a counter-example). This is due, primarily, to two historical inconsistencies in the literature: (1) published equations for $\eta_s(\phi)$ divide into two approximately equally sized groups, one asserting that η_s increases with increasing ϕ, the other that η_s decreases with increasing ϕ; (2) within each group there is little consensus on the functional form of $\eta_s(\phi)$. In recent years, several papers have been published which have addressed both of these deficiencies. Critically, the apparent confusion over the sign of $\eta_s(\phi)$ has been resolved: bubbles can either increase or decrease the shear viscosity of a suspension depending on the dynamic regime (Manga et al., 1998; Spera and Stein, 2000; Llewellin et al., 2002a,b; Rust and Manga, 2002a; Stein and Spera, 2002). In addition, some of these studies added new experimental data constraining the functional form of $\eta_s(\phi)$.

Given these advances, it is now possible to include bubble-suspension rheology in conduit-flow and eruption models. The main purpose of this paper is to present an algorithmic approach to including the effects of bubble-suspension rheology in such models: this is intended as a 'how to' guide for modellers. Additionally, we include a brief review of bubble-suspension rheology with a particular emphasis on clarifying the recent advances mentioned above. Some models, described elsewhere in this volume, have already implemented the algorithm presented here and we discuss some results from these models which give an indication of the consequences of bubble-suspension rheology for conduit-flow and eruption models.

2. Bubble suspension rheology

The rheological property of a bubble suspension that is of greatest importance in conduit flow is its shear viscosity η_s. This is typically normalized to the viscosity of the liquid phase μ_0 and presented as the relative viscosity η_r:

$$\eta_r = \frac{\eta_s}{\mu_0}. \tag{1}$$

η_r is a function of the gas volume-fraction ϕ, that may increase or decrease with increasing ϕ depending on the conditions of shear and the bubble-relaxation time λ. The quantity λ is a measure of the timescale over which a bubble can respond to changes in its shear environment. For a single bubble in an infinite medium:

$$\lambda = \frac{\mu_0 a}{\Gamma} \tag{2}$$

where a is the undeformed bubble radius and Γ is the bubble–liquid interfacial tension. There is some evidence that λ is an increasing function of ϕ (Oldroyd, 1953; Oosterbroek and Mellema, 1981; Loewenberg and Hinch, 1996; Llewellin et al., 2002a), however, Rust et al. (2003) show that the dependence of λ on ϕ is rather weak so, for simplicity, it is proposed that Eq. (2) is used for all ϕ. Other aspects of the suspension rheology are also strongly influenced by the presence of bubbles. For example, viscoelastic effects, including recoverable strain, are introduced. In addition, normal stress differences are generated even if the suspending liquid is Newtonian (e.g., Schowalter et al., 1968; Stein and Spera, 1992; Manga et al., 1998). Such effects are not considered further in this paper.

The algorithm for including bubble-suspension rheology in conduit-flow models, which is presented later in Section 3, depends upon distinguishing the two dynamic regimes for $\eta_r(\phi)$. We identify:

Regime 1: shear viscosity increases with increasing gas volume-fraction.
Regime 2: shear viscosity decreases with increasing gas volume-fraction.

The regime can be determined by calculating the capillary number (*Ca*, defined later in Eq. (3)) for a steady flow (Llewellin et al., 2002b; Rust and Manga, 2002a; Stein and Spera, 2002) or the dynamic capillary number (*Cd*, defined later in Eq. (4)) for an unsteady flow (Llewellin et al., 2002a,b) as described in detail below.

2.1. Steady flows

A flow is described as "steady" if the conditions of shear have remained constant (in the Lagrangian sense) for a time before present $t \gg \lambda$ (Llewellin et al., 2002a; Rust and Manga, 2002b). This definition is relaxed somewhat in Section 2.2. Manga and Loewenberg (2001), Llewellin et al. (2002b), Rust and Manga (2002a) and Stein and Spera (2002) show that, for a steady flow, the viscous regime is controlled by the capillary number Ca, given by:

$$Ca = \lambda\dot{\gamma} \tag{3}$$

where $\dot{\gamma}$ is the shear strain-rate. Ca describes the relative importance of viscous stresses (of order $\mu_0\dot{\gamma}$) , which tend to deform the bubbles, and interfacial stresses (of order Γ/a), which tend to restore them to sphericity. Since the flow is steady, Ca refers to the equilibrium between these forces, hence, the bubble shape is also stable (bubbles are described as relaxed) and is referred to as the equilibrium deformation. The magnitude of equilibrium bubble-deformation, therefore, depends on Ca. If $Ca \ll 1$, interfacial tension forces dominate and bubbles are approximately spherical (e.g., Taylor, 1934). If $Ca \gg 1$, viscous forces dominate and bubbles will be elongate (e.g. Hinch and Acrivos, 1980). The effect of bubble shape on viscosity can be explained as follows: Bubbles deform flow lines within the suspending medium, which tends to increase viscosity; bubbles provide free-slip surfaces within the suspending medium, which tends to decrease viscosity. For small Ca (bubbles are almost spherical) flow-line distortion is great and free-slip surface area is small, hence, $\eta_r > 1$; for large Ca (bubbles are elongate) flow-line distortion is small and free-slip surface area is great, hence, $\eta_r < 1$.

In summary: if $Ca \ll 1$, viscosity increases with increasing gas volume-fraction (regime 1); if $Ca \gg 1$, viscosity decreases with increasing gas volume-fraction (regime 2).

In principle, if the shape of bubbles can be determined as a function of Ca and ϕ then the rheology of the suspension can predicted (e.g., Batchelor, 1970). The problem, however, lies in determining bubble shape. For dilute suspensions, analytical results are available for small deformations (e.g., Taylor, 1934) and highly elongate bubbles (e.g., Hinch and Acrivos, 1980). Models are also derived for intermediate deformation (e.g., Wu et al., 2002). In general theoretical results for bubble shape agree well with experimental measurements (e.g., Rust and Manga, 2002b; Hu and Lips, 2003; Yu and Bousmina, 2003). When the suspension is no longer dilute, however, the interactions between bubbles affect their shapes and consequently the rheology. Unfortunately, the rheology can be predicted accurately only if the bubble shape is accurately known (Cristini et al., 2002).

2.2. Unsteady flows

Given the definition of a steady flow at the beginning of Section 2.1, it is clear that, if the shear strain-rate is changing, the flow must be unsteady. In fact, Llewellin et al. (2002a,b) have shown that there are degrees of steadiness of flow which can be described using the dynamic capillary number Cd, given by:

$$Cd = \lambda\frac{\ddot{\gamma}}{\dot{\gamma}} \tag{4}$$

where $\ddot{\gamma}$ is the rate of change of shear strain-rate. Cd compares the timescale over which the bubbles can respond to changes in their shear environment (the bubble-relaxation time λ) with the timescale over which the shear environment changes (of order $\dot{\gamma}/\ddot{\gamma}$). If $Cd \ll 1$, the bubbles are able to respond continuously to the changes in shear environment. Consequently, the bubbles are always approximately in their equilibrium deformation and the flow is approximately steady. Since the flow is approximately steady, the dynamic regime is controlled by the capillary number Ca as described in Section 2.1. If, however, $Cd \gg 1$, the shear environment is changing too rapidly for the bubbles to respond, therefore the bubbles are unrelaxed. Since the bubbles never reach their equilibrium deformation, Ca is undefined and the flow is described as unsteady. In an unsteady flow, the bubbles do not have time to respond elastically to changes in shear, hence, they behave as if they have no bubble–liquid interfacial tension. Since there is, effectively, no elastic force affecting the shape of the bubbles, their response to the local shearing of the suspending liquid is purely viscous and, since they have negligible viscosity, they deform passively with the suspending liquid. This decreases the distortion of flow-lines around the bubbles leading to a decrease in

the viscosity of the suspension as ϕ increases (Llewellin et al., 2002a).

In summary: if $Cd \ll 1$, flow is approximately steady so regime is determined by considering Ca; $Cd \gg 1$ denotes unsteady flow and viscosity decreases with increasing gas volume-fraction (regime 2).

Just as rheology can be calculated from knowledge of bubble shapes for steady flows, so too can the rheology for unsteady flows if the evolution of bubble shape is known (e.g., Tucker and Moldenaers, 2002). Several recent studies have made progress in developing models for the time-dependent deformation of bubble shape and rheology in a variety of flow geometries (e.g., Maffettone and Minale, 1998; Jansseune et al., 2001; Jackson and Tucker, 2003; Yu and Bousmina, 2003).

2.3. Proposed rheological model

There are nine published datasets from laboratory experiments on bubble suspensions (Rahaman et al., 1987; Ducamp and Raj, 1989; Bagdassarov and Dingwell, 1992, 1993; Stein and Spera, 1992, 2002; Lejeune et al., 1999; Llewellin et al., 2002a; Rust and Manga, 2002a). Of these, unsteady flows are considered explicitly in the studies of Bagdassarov and Dingwell (1993) and Llewellin et al. (2002a). From the published experimental details it is possible to deduce that the data presented in Rahaman et al. (1987), Ducamp and Raj (1989), Bagdassarov and Dingwell (1992), Lejeune et al. (1999), and Stein and Spera (2002) where collected from unsteady flows. Rust and Manga (2002a) explicitly considered steady flow. In addition, there are two published datasets from numerical models of bubble suspensions (Manga et al., 1998; Manga and Loewenberg, 2001). Many of the papers mentioned above present models for $\eta_r(\phi)$ based on their experimental data. These and other models are discussed in detail in Llewellin et al. (2002a).

From the data it is evident that $\eta_r(\phi)$ is largely independent of Cx (where Cx represents either Ca or Cd) when $Cx \ll 1$ and $Cx \gg 1$. $\eta_r(\phi)$ is strongly dependent on Cx only in the narrow region where the dynamic regime changes ($Cx \approx O(1)$). Additionally, in this region, no easily evaluated equation for $\eta_r(\phi,Cx)$ has been published. For these reasons, we propose that $\eta_r(\phi,Cx)$ should be treated as a step-function, with one equation for $\eta_r(\phi)$ used for $Cx \leq 1$ (regime 1) and another equation for $\eta_r(\phi)$ used for $Cx > 1$ (regime 2). This approach significantly simplifies the task of including bubble-suspension rheology in numerical models whilst retaining its most important features. An indication of the size of the error in η_r which is introduced in the region where $Cx \approx O(1)$ by this approximation is presented in Fig. 1, which compares the curve of $\eta_r(Ca)$ (for ϕ=0.4 and steady flow) produced by the "model 4" of Pal (2003) (presented below as Eq. (5)) and the simplified model

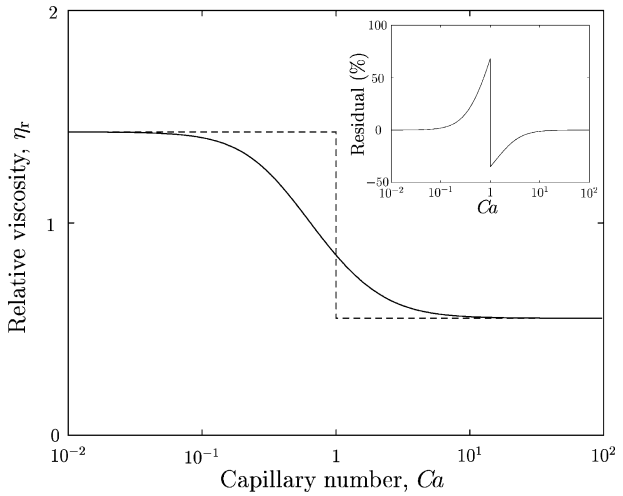

Fig. 1. Comparison of $\eta_r(Ca)$ calculated using "model 4" of Pal (2003) (solid line) and using the simplified model proposed in this paper (dashed line) for ϕ=0.4. Inset shows residual as a percentage of the value calculated using Pal's equation.

proposed in this paper. It is argued that the residual is acceptable when it is considered that, in a volcanic eruption, values of Cx will span many orders of magnitude and the transition through $Cx \approx O(1)$ is likely to be very rapid in space and time.

Llewellin et al. (2002b) show that $\eta_r(\phi,Ca)$ and $\eta_r(\phi,Cd)$ are identical (that is, the dependence of shear viscosity on gas volume-fraction is identical for both steady and unsteady flows) except for a very small deviation when $Cx \approx 1$. We propose, therefore, that a single equation for the positive dependence of η_r on ϕ is used for regime 1 and a single equation for the negative dependence of η_r on ϕ is used for regime 2, regardless of whether regime 2 behaviour is due to $Ca>1$ (for a steady flow) or $Cd>1$ (for an unsteady flow).

We must now choose a physical model for $\eta_r(\phi)$ to be used for regime 1 and another for regime 2. Pal (2003) presents four semi-empirical models for $\eta_r(\phi,Ca)$ for steady flows, parameterized using previously published data for the rheology of bubble suspensions. He obtains the best fit to data using his "model 4":

$$\eta_r \left(\frac{1 - \frac{12}{5}\eta_r^2 Ca^2}{1 - \frac{12}{5} Ca^2} \right)^{-\frac{4}{5}} = \left(1 - \frac{\phi}{\phi_m} \right)^{-\phi_m} \qquad (5)$$

where ϕ_m is the maximum packing fraction of bubbles. This model is an extension, after the method of Brinkman (1952) and Roscoe (1952), of the Frankel and Acrivos (1970) model, to non-dilute suspensions. In this form, Eq. (5) is quadratic in η_r, hence it has two possible solutions making the equation's practical implementation in a conduit-flow model difficult. The introduction of a maximum packing fraction (by analogy with the Brinkman–Roscoe method for suspensions of solid particles) is also somewhat problematic: since bubbles are deformable, no clear maximum packing fraction exists (except, perhaps, $\phi_m=1$). Since no real solution to Eq. (5) exists for $1>\phi \geq \phi_m$ and ϕ may approach unity in an erupting magma, the most reasonable course is always to set $\phi_m=1$. In this case, for the limits of large and small Ca, Eq. (5) reduces to:

$$\eta_r = \begin{cases} (1-\phi)^{-1} : Ca \ll 1 \\ (1-\phi)^{\frac{5}{3}} \ : Ca \gg 1. \end{cases} \qquad (6)$$

Pal's model does not consider the steadiness of the flow, a property which has been shown by Llewellin et al. (2002a,b) to be a fundamental control on the rheology of a bubble suspension in the flows that arise in volcanic conduits. However, since Llewellin et al. (2002b) also show that $\eta_r(\phi,Cx)$ is almost identical for steady and unsteady flows it is reasonable to assume that Eq. (6) has equal validity for unsteady flows (with Cd replacing Ca for each regime).

For experimental and numerical investigations of bubble suspensions in regime 1: Eq. (6) is compatible with Manga et al. (1998), Rust and Manga (2002a) and with Llewellin et al. (2002a) for $0<\phi<0.07$. The model is incompatible with data from Llewellin et al. (2002a) for $\phi>0.07$ or Stein and Spera (1992), both of which indicate a much stronger positive dependence of η_r on ϕ than predicted by Pal's model.

For experimental and numerical investigations of bubble suspensions in regime 2: Eq. (6) is compatible with Lejeune et al. (1999), Manga and Loewenberg (2001), Stein and Spera (2002) and Llewellin et al. (2002a), most of whom considered simple shearing flows. The model is incompatible with data from sintering experiments and extensional flows (Rahaman et al., 1987; Ducamp and Raj, 1989; Bagdassarov and Dingwell, 1992), all of which indicate a much stronger negative dependence of η_r on ϕ than predicted by Pal's model. Possibly a volume change in these latter experiments may have influenced their results.

It is clear from the above that the "model 4" proposed by Pal does not capture the behaviour identified in several experimental studies of bubble suspension behaviour. However, it does capture the broad trends which exist in all of the data (steady and unsteady) in both regimes. In addition, the model tends to underestimate the importance of bubbles in controlling the shear viscosity of a suspension in both regimes. The model can, therefore, be usefully employed as a 'minimum' model of bubble rheology and the effect of bubbles on conduit-flow dynamics in the real world will be at least as great as any effect identified using a conduit-flow model which incorporates the effect of bubbles on rheology using this model. Bearing in mind the simplifying assumption, presented above, that regime 1 extends to $Cx \leq 1$ and regime 2 from $Cx>1$, we, therefore, propose the

following minimum model of bubble-suspension rheology for use in conduit-flow models:

$$\text{Regime 1 (min.)} : \eta_r = (1-\phi)^{-1}, \quad (7)$$

$$\text{Regime 2 (min.)} : \eta_r = (1-\phi)^{\frac{5}{3}}. \quad (8)$$

Note that Eqs. (7) and (8) reduce to the exact analytical results for dilute ($\phi \ll 1$) suspensions for both regime 1 (Taylor, 1932) and regime 2 (Mackenzie, 1950).

It is also of interest to investigate a 'maximum' model of bubble rheology, based on models for behaviour in regimes 1 and 2 proposed by those workers who find a stronger dependence of η_r on ϕ than is predicted by Eqs. (7) and (8). For regime 1, the strongest dependence is proposed by Llewellin et al. (2002a):

$$\text{Regime 1 (max.)} : \eta_r = 1 + 9\phi. \quad (9)$$

This relationship is based on experiments on bubble suspensions in the range $0 \leqslant \phi \leqslant 0.5$. For regime 2, we propose that the model presented by Bagdassarov and Dingwell (1992) is used:

$$\text{Regime 2 (max.)} : \eta_r = \frac{1}{1 + 22.4\phi}. \quad (10)$$

This equation is based on measurements of bubble suspensions in the range $0 \leqslant \phi \leqslant 0.7$. It is probable that the true effect of bubbles on conduit-flow dynamics will be somewhere between that predicted using the minimum and maximum models presented above.

3. Implementation of bubble-suspension rheology

We propose that conduit-flow models incorporate the effect of bubbles on rheology by first calculating the dynamic regime of the flow in each conduit element, then calculating the viscosity of the material in that conduit element using Eq. (7) for flows in regime 1 and Eq. (8) for flows in regime 2 when using the minimum model and Eqs. (9) and (10) when the maximum model is employed—see Section 2.3. The procedure is summarized in Fig. 2. It is envisaged that the viscosity determination will occur at the end of each timestep for each conduit element. The resulting viscosity value will then be used to determine the velocity profile in the next timestep.

To calculate Ca (Eq. (3)) and Cd (Eq. (4)), the relaxation time λ, the shear strain-rate $\dot{\gamma}$ and the rate of change of shear strain-rate $\ddot{\gamma}$ must first be calculated. The remainder of this section describes how these quantities may be calculated for a one-dimensional conduit-flow model.

3.1. Calculating the relaxation time λ

Relaxation time is given by Eq. (2), represented below for convenience:

$$\lambda = \frac{\mu_0 a}{\Gamma}.$$

Due to decompressive and diffusive growth of bubbles, λ changes over time as a packet of magma ascends, hence it must be calculated for each conduit element in the model at each timestep. μ_0 is the viscosity of the liquid part of the two-phase material at that point (i.e. the melt viscosity, usually calculated from composition and temperature of the silicate melt). Γ is the liquid–bubble interfacial tension at that point; a value of ≈ 0.25 N m^{-1} can be deduced from Fig. 31 of Murase and McBirney (1973).

The undeformed bubble radius a (the radius of a spherical bubble of equal volume), may be calculated explicitly in some conduit-flow models, but not in others. If a is ordinarily calculated, the value appropriate for that element at that timestep should be used. If a is not ordinarily calculated, it may be determined from the gas volume-fraction by assuming a bubble number-density at nucleation (see table of model parameters elsewhere in this volume) and assuming some function for bubble number-density with time: e.g. bubble number-density (with respect to the volume of the liquid part of the suspension) over time remains constant.

3.2. Calculating the shear strain-rate $\dot{\gamma}$

The shear strain-rate must be calculated for each conduit element at each timestep. For laminar, uniaxial flow along a conduit, the velocity $\boldsymbol{u}=[u_z(r), 0, 0]$ as shown in Fig. 3. For such a flow, the shear strain-rate is given by:

$$\dot{\gamma} = \left| \frac{\mathrm{d}u_z}{\mathrm{d}r} \right| \quad (11)$$

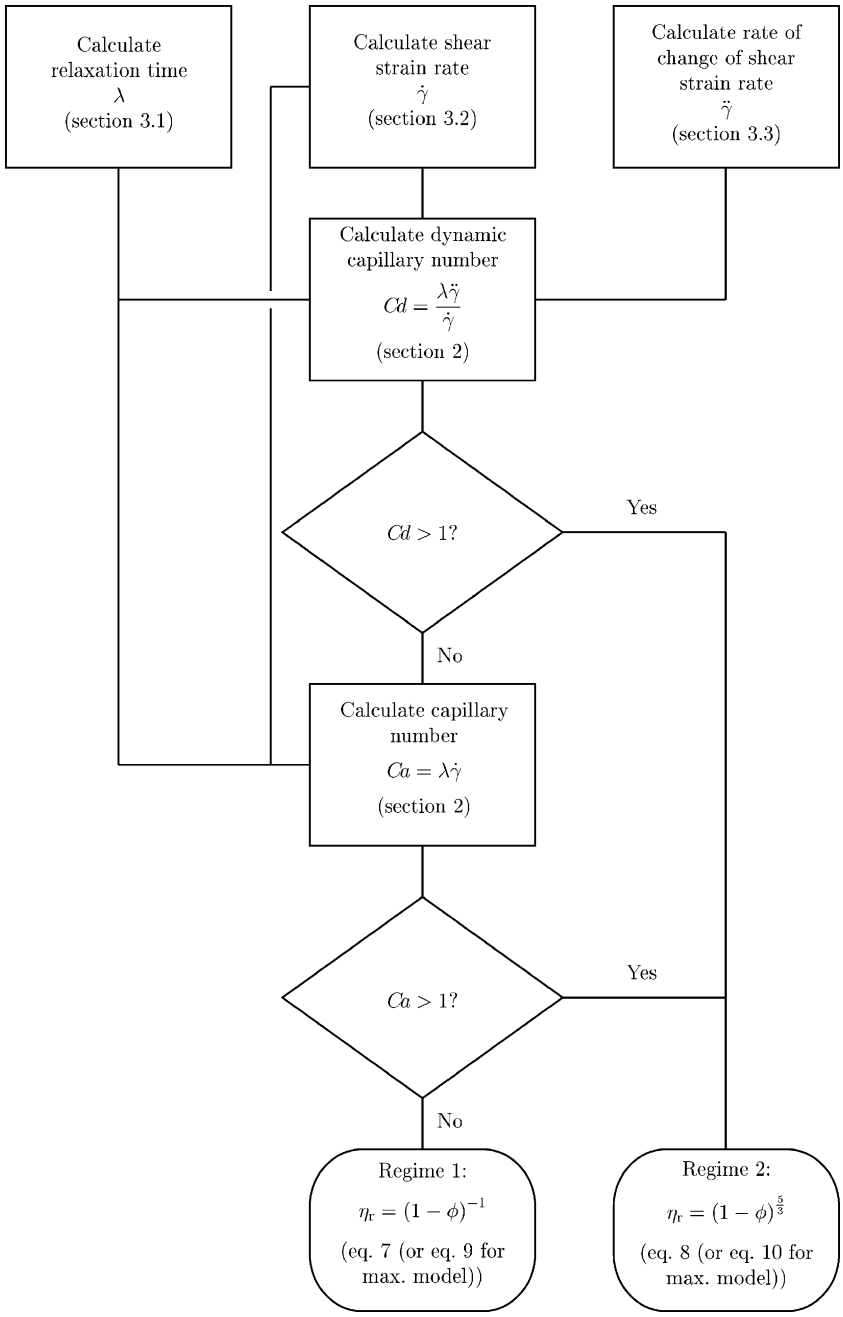

Fig. 2. Flowchart showing algorithm for determination of shear viscosity of bubbly magma for each conduit element. Comments in brackets refer to sections and equations in the main text. For explanation of 'maximum' models, see Section 2.3.

hence shear strain-rate is a function of radial position in the conduit. It is not possible to calculate $u_z(r)$ using a one-dimensional conduit-flow model so, in order to calculate $\dot{\gamma}$, a velocity profile must be assumed.

For slow, steady flows, the shear strain-rate will be low at all points across the conduit, hence $Ca<1$ everywhere. The viscosity of the bubble suspension will, consequently, be the same everywhere so the

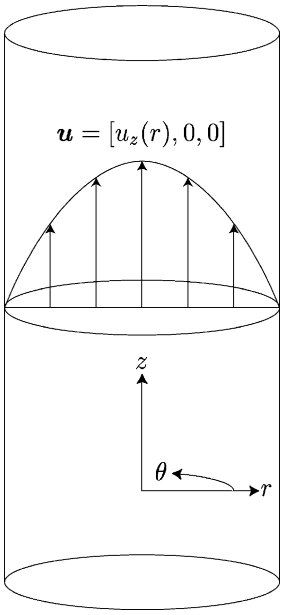

Fig. 3. Conduit flow.

velocity profile will be parabolic (the bubble suspension will behave as a Newtonian liquid with a viscosity given by the equation for regime 1 (Eq. (7), min. model, or (9), max. model). For a parabolic velocity profile, the shear strain-rate varies from zero at the axis to a maximum at the conduit wall. For a bubble suspension, this leads to an interesting phenomenon as the flow rate increases: whilst the shear strain-rate at the axis remains low (hence $Ca<1$), the shear strain-rate near the conduit wall may increase to the point where $Ca>1$. In this configuration, at all points axial of the transition, the viscosity of the bubble suspension will be given by the equation for regime 1 but, radially outwards from the transition, the viscosity will be lower, given by the equation for regime 2 (Eq. (8), min. model, or (10), max. model). This leads to a non-parabolic velocity profile as shown in Llewellin et al. (2002b). At still higher flow rates, the shear strain-rate across most of the conduit is such that $Ca>1$ except for a narrow region near the axis and the velocity profile is, again, approximately parabolic. Unfortunately, this transitional behaviour can only be captured by 2d and 3d flow models, however, Llewellin et al. (2002b) show that, in their 2d, steady-flow model, significant departure from parabolic flow occurs only for a narrow range of conditions, hence it is reasonable, for the purposes of this exercise, to assume that the velocity profile in the conduit is always parabolic. Where the velocity profile can be calculated explicitly (in certain 2d and 3d models), local shear strain-rate, and therefore local capillary numbers and local viscosity, can be calculated at points across the conduit element, allowing more accurate implementation of bubble-suspension rheology (e.g., Gonnermann and Manga, 2003).

Given a parabolic velocity profile, it is possible to calculate an average shear strain-rate in terms of the volume flow-rate Q, the average velocity $\hat{u}_z$ or the axial velocity u_0 (depending on which is calculated by the conduit-flow model). The average shear strain-rate can then be used to calculate the capillary number and hence the viscosity of the bubble suspension under those conditions of shear.

Assuming a parabolic velocity profile across the conduit we obtain:

$$u_z = u_0\left(1 - \frac{r^2}{R^2}\right) \tag{12}$$

where r is the radial position in the conduit and R is the radius of the conduit (assuming no slip at the conduit wall: $u_z=0$ at $r=R$). Integrating across the conduit gives the volume flow-rate:

$$Q = 2\pi u_0 \int_0^R r\left(1 - \frac{r^2}{R^2}\right)\mathrm{d}r \tag{13}$$

hence

$$u_0 = \frac{2Q}{\pi R^2}. \tag{14}$$

Volume flow-rate is the product of the average velocity and the cross-sectional area of the conduit, hence:

$$\hat{u}_z = \frac{Q}{\pi R^2}. \tag{15}$$

We can see from Eqs. (14) and (15) that the axial velocity for parabolic flow along a pipe is twice the average velocity:

$$u_0 = 2\hat{u}_z. \tag{16}$$

Substituting Eq. (14) into Eq. (12):

$$u_z = \frac{2Q}{\pi R^2}\left(1 - \frac{r^2}{R^2}\right). \tag{17}$$

Applying Eq. (11) to the above we obtain the shear strain-rate as a function of radial position in the conduit:

$$\dot{\gamma} = \frac{4\hat{u}_z r}{R^2}. \tag{18}$$

Integrating across the conduit and dividing by the cross-sectional area, we obtain the average shear strain-rate:

$$\hat{\dot{\gamma}} = \frac{8\hat{u}_z}{R^4}\int_0^R r^2 \mathrm{d}r \tag{19}$$

which, using Eqs. (15) and (16), can be expressed in terms of the average velocity, the axial velocity or the volume flow-rate, hence, the average shear strain-rate can be calculated for each conduit element (the ^ is dropped for convenience):

$$\dot{\gamma} = \frac{8\hat{u}_z}{3R} = \frac{4u_0}{3R} = \frac{8Q}{3\pi R^3}. \tag{20}$$

3.3. Calculating the rate of change of shear strain-rate $\ddot{\gamma}$

The rate of change of shear strain-rate must be calculated for each conduit element at each timestep. Note that this is the rate of change of shear strain-rate experienced by a packet of the magma as it rises up the conduit hence, even for a 'steady' model in which the velocity profile up the conduit does not change with time, the shear strain-rate experienced by a rising packet of magma does change over time.

The rate of change of shear strain-rate $\ddot{\gamma}$ can be estimated by considering the strain-rate in adjacent elements of the conduit (Fig. 4). It is assumed that, for each element i of the flow, at depth z_i, the axial velocity u_{0_i} (or the average velocity $\hat{u}_{z_i}$ or the volume flow-rate Q_i—see Eq. (20)) is known, hence, the shear strain-rate $\dot{\gamma}_i$ can be calculated according to the method described in Section 3.2. The rate of change of shear strain-rate for a packet of material is approximately given by:

$$\ddot{\gamma} \approx \frac{\Delta\dot{\gamma}}{\Delta t} \tag{21}$$

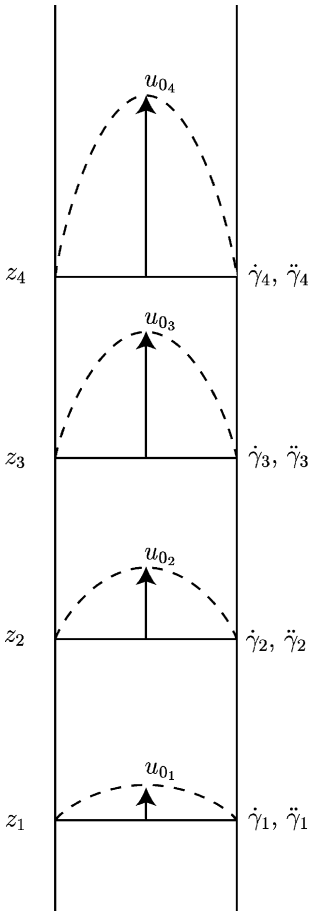

Fig. 4. Conduit elements.

where $\Delta\dot{\gamma}$ is the change in shear strain-rate experienced by the packet over time Δt. In Fig. 4 material at element i is arriving from element $i-1$, hence it has experienced a change in shear strain-rate given by:

$$\Delta\dot{\gamma}_i = \dot{\gamma}_i - \dot{\gamma}_{i-1}. \tag{22}$$

The time taken for the material to undergo this change is approximately the quotient of the distance between the elements and the average flow velocity between the elements:

$$\Delta t = \frac{2(z_i - z_{i-1})}{\hat{u}_{z_i} + \hat{u}_{z_{i-1}}} \tag{23}$$

hence:

$$\ddot{\gamma}_i \approx \frac{(\dot{\gamma}_i - \dot{\gamma}_{i-1})(\hat{u}_{z_i} + \hat{u}_{z_{i-1}})}{2(z_i - z_{i-1})} \tag{24}$$

where all quantities are evaluated in the current timestep and where the average velocity can be derived from the axial velocity or the volume flow-rate using Eqs. (15) and (16). The dynamic capillary number for element i is, therefore, given by:

$$Cd_i = \lambda \frac{\ddot{\gamma}_i}{\dot{\gamma}_i}. \quad (25)$$

4. Volcanological implications of including bubble-suspension rheology

Our proposed model implies that, for a gas volume-fraction of ϕ<0.5, η_r can differ between the two regimes by up to a factor of 5 for the minimum model and a factor of 70 for the maximum model. The magnitude of this effect is thus small compared to viscosity changes that ascending magmas can experience due to crystallization and the loss of volatiles. Nevertheless, there is some preliminary evidence that the change in viscosity due to the presence of bubbles has a significant effect on the predictions of conduit-flow models. In Fig. 5 we show, for example, the predictions of the CONFLOW model (Mastin, 2002) for three cases: (1) the effect of bubbles is not considered; (2) bubbles are considered and flow is assumed to be in regime 1 (minimum model) throughout the conduit; (3) flow is assumed to be in regime 2 (minimum model) throughout the conduit. All other parameters are the same for all three calculations. Despite using the minimum rheological model, the inferred fragmentation depth for these three cases varies by ≈800 m, indicating that the influence of bubbles on fragmentation depth in a natural eruption is at least this strong and may be much stronger.

Elsewhere in this volume, Starostin et al. (this issue) present a conduit-flow model which calculates the effect of bubbles on rheology after the method proposed in this paper. Unlike the CONFLOW model (Mastin, 2002), the model of Starostin et al. (2005-this issue) calculates both capillary numbers for the flow in each conduit element, determines the viscous regime and applies the appropriate viscosity equation. Fig. 6 shows the predictions of this model for three cases: (1) the effect of bubbles is not considered; (2) bubbles

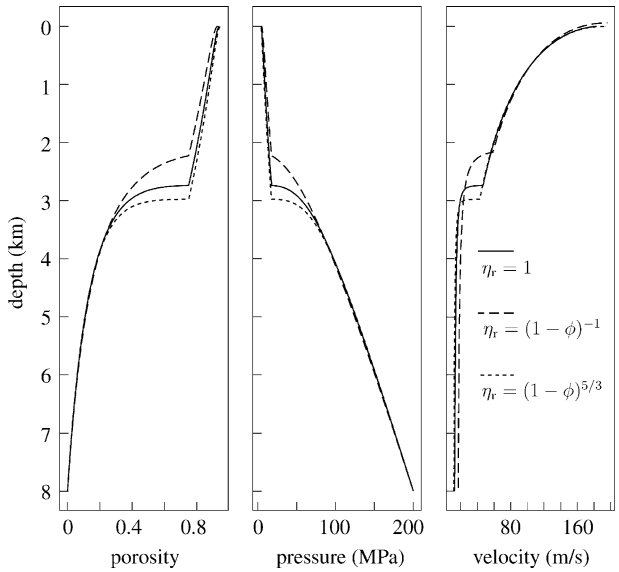

Fig. 5. Porosity, pressure and vertical velocity against depth in a volcanic conduit calculated using CONFLOW (Mastin, 2002) with a magma chamber depth of 8 km. The solid line ignores the effect of bubbles on viscosity, the dashed line illustrates the effect of bubbles under the assumption that flow is in regime 1 (minimum model) throughout the conduit, the dotted line illustrates the effect of bubbles under the assumption that flow is in regime 2 (minimum model) throughout the conduit. In each case the fragmentation depth is indicated by the inflection point in the curve. It can be seen that, even for the minimum rheological model employed here, accounting for bubble-suspension rheology has a clear influence on fragmentation depth.

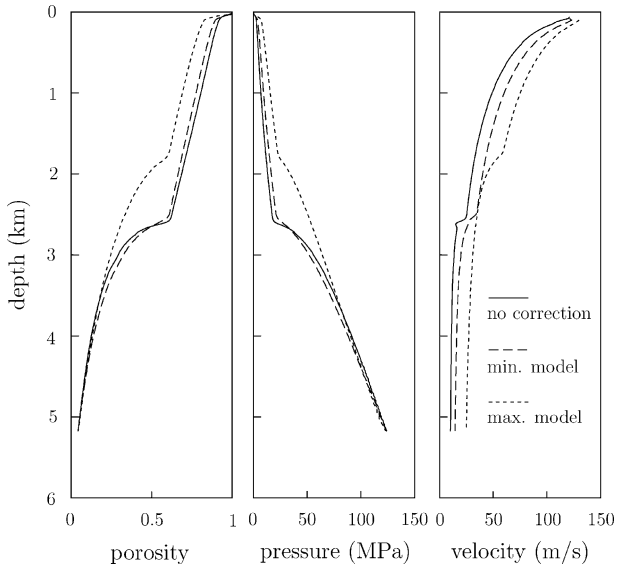

Fig. 6. Porosity, pressure and vertical velocity against depth in a volcanic conduit calculated using the model of Starostin et al. (2005-this issue) with a magma chamber depth of 5.2 km and a conduit radius of 25 m. The solid line ignores the effect of bubbles on viscosity, the dashed line illustrates the effect of bubbles assuming the minimum rheological model, the dotted line illustrates the effect of bubbles assuming the maximum rheological model. In each case the fragmentation depth is indicated by the inflection point in the curve. This model predicts that the effect of including bubble-suspension rheology on the conduit parameters shown is small when using the minimum model, however, when using the maximum model, a change in fragmentation depth of 800 m is predicted.

considered and the minimum model is used (Eqs. (7) and (8)); (3) bubbles are considered and the maximum model is used (Eqs. (9) and (10)). In all cases, the values presented are calculated after the model eruption has reached steady state. Note that this model is more sophisticated than the CONFLOW model in its handling of bubble-suspension rheology and the viscous regime changes with position in the conduit (i.e. the bubbles may increase or decrease the viscosity of the mixture depending on the local values of the capillary numbers).

Fig. 6 shows that, whilst the effect of including bubble-suspension rheology on the model predictions is negligible when applying the minimum model, when the maximum model is applied, a decrease in fragmentation depth of 800 m is predicted. Furthermore, the upward velocity of the magma is markedly increased when the maximum model is used, compared with the value predicted when the effect of bubbles is not considered. This increase in upward velocity is linked to a dramatic increase in the discharge rate predicted when the effect of bubbles on magma rheology is considered. This effect is illustrated in Fig. 7 which shows the discharge rate (volume erupted per unit time) as a function of time for the same three cases (no bubbles; minimum model; maximum model) and the same starting conditions as shown in Fig. 6. This figure shows that the model of Starostin et al. (2005-this issue) predicts an increase in eruption rate of between 40% and 250% when the effect of bubbles on rheology is considered compared to when it is not, depending on whether the minimum or maximum model is used. This result shows that accounting for the effect of bubbles on magma rheology in a conduit-flow model can have a significant effect on the model's predictions. In particular, models which ignore the effect of bubbles on magma rheology may be significantly underestimating discharge rates during an eruption.

It is worth noting that all current eruption and conduit-flow models make many simplifying assumptions, typically one or more of the following: 1d or 2d flow, radially symmetric conduit, constant conduit cross-section, no viscous dissipation, no slip at conduit walls, laminar flow. Sometimes these assumptions are made to reduce computational load, sometimes they are made because the effect is considered unimportant and some assumptions are made because of a lack of phenomenological evidence. It is likely that some of

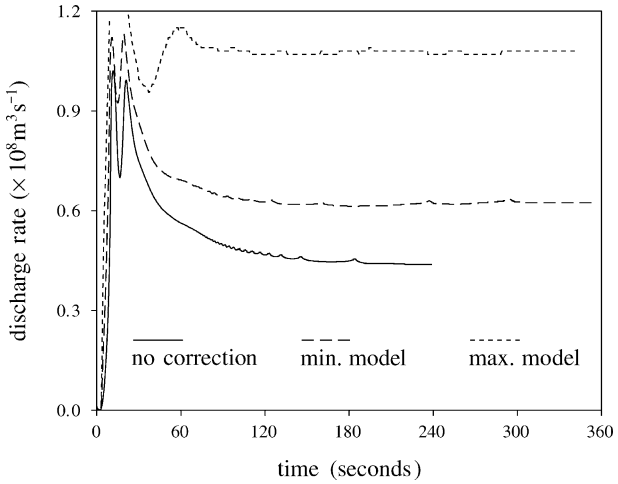

Fig. 7. Discharge rate over time for an explosive eruption using the model of Starostin et al. (2005-this issue) for a magma chamber depth of 5.2 km and a conduit radius of 25 m. The solid line ignores the effect of bubbles on viscosity, the dashed line illustrates the effect of bubbles assuming the minimum rheological model, the dotted line illustrates the effect of bubbles assuming the maximum rheological model. In each case the curve terminates when the model eruption has reached steady state. When the minimum model is used, the steady-state eruption rate predicted is increased by 40% compared with that predicted when the effect of bubbles is ignored; when the maximum model is used, the predicted increase is 250%.

these assumptions have a greater effect on the model's output (and on its accuracy) than the "no bubble-suspension rheology" assumption that prevails in most models. Furthermore, when dealing with a complex, coupled, non-linear system of equations, as all conduit-flow models do, it is difficult to predict what the effect of including another non-linear term (in this case the bubble-suspension rheology) will be. We have shown that, at least in the case of the models used in this study and under the assumption of parabolic velocity profiles, bubble-suspension rheology has a clear impact on the models' predictions. We consider it likely that the predictions of other models, of all levels of sophistication, will be modified to a similar extent by the inclusion of bubble-suspension rheology.

5. Concluding remarks

The conduit model predictions shown in Figs. 5–7 illustrate the impact of accounting for bubble-suspension rheology. We note, however, that both our discussion and current conduit models address only one aspect of the effect of bubbles on conduit-flow dynamics: the effect on shear viscosity. Other effects, such as non-zero normal stresses, introduction of a bulk (compressible) viscosity, bubble coalescence and breakup, etc., may also have a significant effect on conduit-flow dynamics. In addition, some of the subtlety of the effect of bubbles on shear viscosity has been sacrificed for simplicity of implementation. It is believed, however, that the method outlined here captures the salient features of bubble rheology. There is still some disagreement between experimental studies on bubble-suspension rheology, highlighted at the end of Section 2.3; one of the strengths of the implementation presented in these notes is that Eqs. (7)–(10) can be adapted easily as improved experimental data become available.

The algorithmic approach to incorporating the effect of bubbles on the shear viscosity of magma in a conduit-flow model is intended as a guide only. It is expected that some deviation from this procedure will be necessary for certain classes of model.

Acknowledgments

We thank Sasha Starostin and coworkers for generously performing runs of their conduit-flow model on our behalf and for allowing us to use the resulting data. We are grateful to Frank Spera, George Bergantz, Takehiro Koyaguchi and an anonymous reviewer for their thoughtful reviews of this paper and

to Heidy Mader for a helpful informal review during its preparation. EWL acknowledges support via NERC Fellowship NER/I/S/2002/00685. MM was supported by NSF EAR 019296.

References

Bagdassarov, N.S., Dingwell, D.B., 1992. A rheological investigation of vesicular rhyolite. J. Volcanol. Geotherm. Res. 50, 307–322.

Bagdassarov, N.S., Dingwell, D.B., 1993. Frequency dependent rheology of vesicular rhyolite. J. Geophys. Res. 98, 6477–6487.

Batchelor, G.K., 1970. The stress system in a suspension of force-free particles. J. Fluid Mech. 41, 470–545.

Brinkman, H.C., 1952. The viscosity of concentrated suspensions and solutions. J. Chem. Phys. 20, 571.

Cristini, V., Macosko, C.W., Jansseune, T., 2002. A note on the transient stress calculation via numerical simulations. J. Non-Newton. Fluid Mech. 105, 177–187.

Ducamp, V.C., Raj, R., 1989. Shear and densification of glass powder compacts. J. Am. Ceram. Soc. 72, 798–804.

Frankel, N.A., Acrivos, A., 1970. The constitutive equation for a dilute emulsion. J. Fluid Mech. 44, 65–78.

Gonnermann, H.M., Manga, M., 2003. Explosive volcanism may not be an inevitable consequence of magma fragmentation. Nature 426, 432–435.

Hinch, E.J., Acrivos, A., 1980. Long slender drops in a simple shear flow. J. Fluid Mech. 98, 305–328.

Hu, Y.T., Lips, A., 2003. Transient and steady state three-dimensional drop shapes and dimensions under planar extensional flow. J. Rheol. 47, 349–369.

Jackson, N.E., Tucker, C.L., 2003. A model for large deformation of an ellipsoidal droplet with interfacial tension. J. Rheol. 47, 659–682.

Jansseune, T., Vinckier, I., Moldernaers, P., Mewis, J., 2001. Transient stresses in immiscible polymer blends during start-up flows. J. Non-Newton. Fluid Mech. 99, 167–181.

Lejeune, A.M., Bottinga, Y., Trull, T.W., Richet, P., 1999. Rheology of bubble-bearing magmas. Earth Planet. Sci. Lett. 166, 71–84.

Llewellin, E.W., Mader, H.M., Wilson, S.D.R., 2002a. The rheology of a bubbly liquid. Proc. R. Soc. A 458, 987–1016.

Llewellin, E.W., Mader, H.M., Wilson, S.D.R., 2002b. The constitutive equation and flow dynamics of bubbly magmas. Geophys. Res. Lett. 29 (Art. No. 2170).

Loewenberg, M., Hinch, E.J., 1996. Numerical simulation of a concentrated emulsion in shear flow. J. Fluid Mech. 321, 395–419.

Mackenzie, J.K., 1950. The elastic constants of a solid containing spherical holes. Proc. R. Soc. A 63, 2–11.

Maffettone, P.L., Minale, M., 1998. Equation of change of ellipsoidal drops in viscous flow. J. Non-Newton. Fluid Mech. 78, 227–241.

Manga, M., Loewenberg, M., 2001. Viscosity of magmas containing highly deformable bubbles. J. Volcanol. Geotherm. Res. 105, 19–24.

Manga, M., Castro, J., Cashman, K., Loewenberg, M., 1998. Rheology of bubble-bearing magmas. J. Volcanol. Geotherm. Res. 87, 15–28.

Mastin, L.G., 2002. Insights into volcanic conduit flow from an open-source numerical model. Geochem. Geophys. Geosyst. 3 (Art. No. 1039).

Murase, T., McBirney, R., 1973. Properties of some common igneous rocks and their melts at high temperatures. Geol. Soc. Am. Bull. 84, 3563–3592.

Oldroyd, J.G., 1953. The elastic and viscous properties of emulsions and suspensions. Proc. R. Soc. A 218, 122–132.

Oosterbroek, M., Mellema, J., 1981. Linear viscoelasticity in emulsions: I. The effect of an interfacial film on the dynamic viscosity of nondilute emulsions. J. Colloid Interface Sci. 8, 14–26.

Pal, R., 2003. Rheological behaviour of bubble-bearing magmas. Earth Planet. Sci. Lett. 207, 165–179.

Rahaman, M.N., De Jonghe, L.C., Scherer, G.W., Brook, R.J., 1987. Creep and densification during sintering of glass powder compacts. J. Am. Ceram. Soc. 70, 766–774.

Roscoe, R., 1952. The viscosity of suspensions of rigid spheres. Br. J. Appl. Phys. 2, 267–269.

Rust, A.C., Manga, M., 2002a. Effects of bubble deformation on the viscosity of dilute suspensions. J. Non-Newton. Fluid Mech. 104, 53–63.

Rust, A.C., Manga, M., 2002b. Bubble shapes and orientations in low Re simple shear flow. J. Colloid Interface Sci. 249, 476–480.

Rust, A.C., Manga, M., Cashman, K.V., 2003. Determining flow type, shear rate and shear stress in magmas from bubble shapes and orientations. J. Volcanol. Geotherm. Res. 122, 111–132.

Schowalter, W.R., Chaffey, C.E., Brenner, H., 1968. Rheological behaviour of a dilute emulsion. J. Colloid Interface Sci. 26, 152–160.

Spera, F.J., Stein, D.J., 2000. Comment on "Rheology of bubble-bearing magmas" by Lejeune et al.. Earth Planet. Sci. Lett. 175, 327–331.

Starostin, A.B., Barmin, A.A., Melnik, O.E., 2005. A transient model for explosive and phreatomagmatic eruptions. J. Volcanol. Geotherm. Res. 143, 133–151 (this issue).

Stein, D.J., Spera, F.J., 1992. Rheology and microstructure of magmatic emulsions: theory and experiments. J. Volcanol. Geotherm. Res. 49, 157–174.

Stein, D.J., Spera, F.J., 2002. Shear viscosity of rhyolite–vapour emulsions at magmatic temperatures by concentric cylinder rheometry. J. Volcanol. Geotherm. Res. 113, 243–258.

Taylor, G.I., 1932. The viscosity of a fluid containing small drops of another fluid. Proc. R. Soc. A 138, 41–48.

Taylor, G.I., 1934. The formation of emulsions in definable fields of flow. Proc. R. Soc. A 146, 501–523.

Tucker, C.L., Moldenaers, P., 2002. Microstructural evolution in polymer blends. Annu. Rev. Fluid Mech. 34, 177–210.

Wu, Y., Zinchenko, A.Z., Davis, R.H., 2002. Ellipsoidal model for deformable drops and application to nonNewtonian emulsion flow. J. Non-Newton. Fluid Mech. 102, 281–298.

Yu, W., Bousmina, M., 2003. Ellipsoidal model for droplet deformation in emulsions. J. Rheol. 47, 1011–1039.